Journal of
Synchrotron
Radiation

ISSN 0909-0495

Received 29 August 2011
Accepted 30 January 2012

An optimized side-cooling scheme for a collimation mirror at the SSRF

Zhongmin Xu and Naxiu Wang*

Department of Beamline Engineering, Shanghai Institute of Applied Physics, Chinese Academy of Sciences, 239 Zhangheng Road, Pudong District, Shanghai 201204, People's Republic of China.
E-mail: wangnaxiu@sinap.ac.cn

Here, in order to reduce tangential slope errors along the centreline of a first mirror's surface, a side-cooling scheme is proposed. The length of the contact area between the mirror and cooling blocks should be smaller than the beam footprint along the mirror. By optimizing the length and the height of the contact area, reduced slope errors can be obtained. Using this scheme the maximum temperature is not located at the centre of the footprint but shifts to both sides, which fundamentally changes the temperature distribution and enhances the cooling effect compared with the traditional method. This paper presents a 'design of experiment' analysis for four kinds of cooling schemes. The structure of the mechanical clamps is also described.

Keywords: side-cooling; thermal analysis; slope error.

1. Introduction

Usually, the first mirror in a synchrotron radiation beamline is subjected to a high heat load from the X-ray source. Surface deformation induced by the heat load degrades the mirror performance. To judge the influence of the heat load on the mirror performance we adopt the criterion of the tangential slope error along the centreline of the mirror. In order to reduce these slope errors, two schemes, internal cooling and contact side-cooling (Khounsary *et al.*, 1998; Jaski *et al.*, 1998; Li *et al.*, 2004; Zhang *et al.*, 2003; Artemev *et al.*, 2001; Lee *et al.*, 2000), can be selected. Although most mirrors work well using these schemes, they are ineffective in some cases. It is found that the slope errors are large when large temperature gradients remain in the tangential direction in the footprint. Moreover, if the maximum temperature is located at the centre of the footprint, large temperature gradients are likely.

In order to decrease these temperature gradients, this article proposes a side-cooling scheme, where the length of the contact area between the mirror and cooling blocks is smaller than the footprint length along the mirror. Minimum slope errors can be obtained by optimizing the length and the height of the contact area. A finite-element analysis for a collimation mirror using ANSYS *Workbench* (ANSYS Inc., 2005) was used to study this approach.

2. Finite-element model

Fig. 1 shows a three-dimensional model of a collimation mirror made of single-crystal silicon and cooling blocks made of OFHC copper, whose material parameters are shown in Table 1. The dimensions of the mirror are 30 mm (X) × 250 mm (Y) × 25 mm (Z). When the X-ray energy is 250 eV, the maximum power and power density absorbed by the mirror are 85.7 W and 0.13 W mm^{-2}, respectively. The centre of the footprint [3 mm (X) × 230 mm (Y)] is coincident with that of the reflecting surface on the mirror; the power density distribution on the mirror is shown in Fig. 2. The equivalent film coefficient between mirror and cooling block is 3.0 × 10^{-3} W mm^{-2} K^{-1} and the reference temperature is 303 K.

Table 1
Material properties of Si and OFHC.

	Young's modulus (GPa)	Thermal conductivity (W m^{-1} K^{-1})	Specific heat (J kg^{-1} K^{-1})	Density (kg m^{-3})	Thermal expansion coefficient (10^{-6} K^{-1})	Poisson ratio
Si	110	148	702	2329	2.2	0.28
OFHC	115	391	385	8900	17.7	0.32

3. Optimization design

As mentioned above, the length and height of the contact area are parameterized and designated as design variables LENGTH and HEIGHT, respectively, whose boundaries are listed in Table 2. The maximum tangential slope error along the mirror centreline acts as an objective function, MaxYSlopeError. An optimization design is performed using the ANSYS *DesignXplorer* module within the ANSYS *Workbench*.

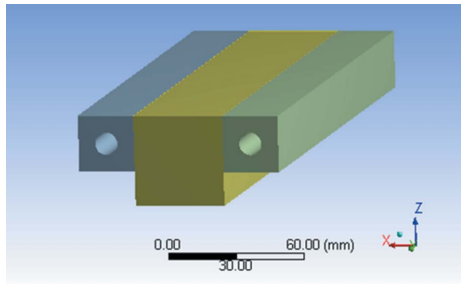

Figure 1
Three-dimensional illustration of the mirror and copper cooling blocks.

Table 2
Design variables boundaries.

Variable name	Lower limit (mm)	Upper limit (mm)
LENGTH	180	250
HEIGHT	2	10

After optimization, a response surface plot (shown in Fig. 3) is obtained. It is helpful to rate the objective function sensitivity based on changes in the design variables. From these plots it can be seen that MaxYSlopeError always increases when HEIGHT varies from 2 mm to 10 mm; there is a minimum for MaxYSlopeError when LENGTH varies from 180 to 250 mm. Because the temperature will rise and result in non-linear effects that increase slope errors when HEIGHT is 2 mm, the height of the contact area cannot be too small. The final scheme is selected where HEIGHT is 6 mm and LENGTH is 215 mm.

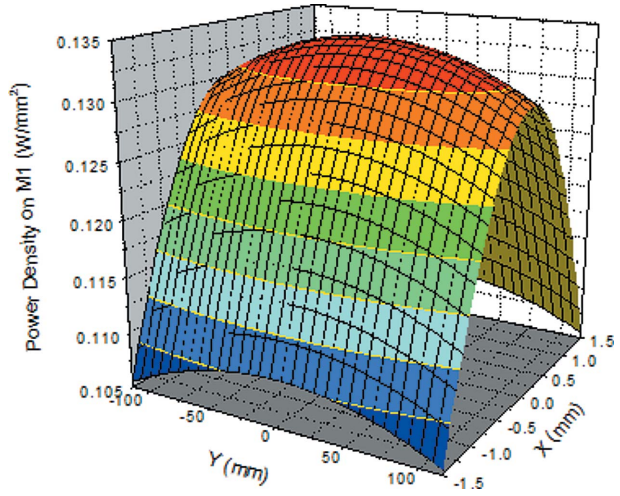

Figure 2
Power density distribution on the mirror.

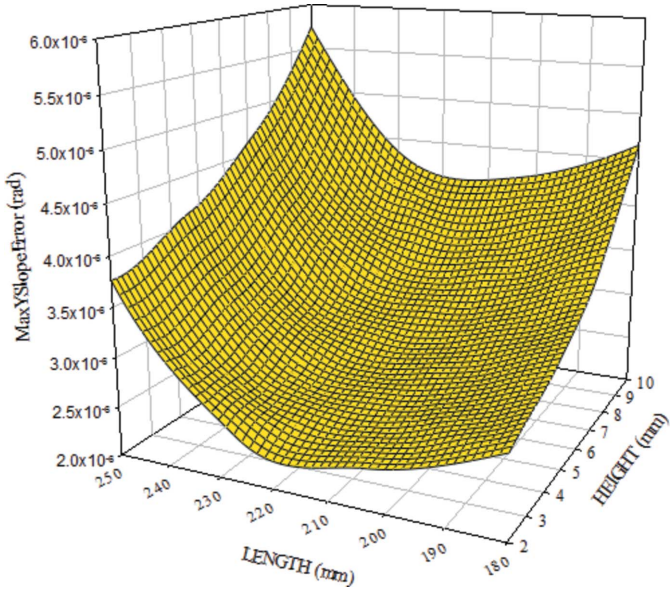

Figure 3
Response surface plot for design variables *versus* maximum tangential slope error.

Table 3
The four different cooling schemes used.

Scheme	Height (mm)	Length (mm)
A	10	250
B	10	205.56
C	9	187.2
D	6	215

4. Comparison between different cooling schemes

In order to analyze how the size of the contact area affects slope errors, four schemes, *A*, *B*, *C* and *D*, shown in Table 3, have been chosen. Scheme *A* is a traditional method where the length of the contact area and mirror is equal. In schemes *B*, *C* and *D* the length of the contact area is smaller than that of the footprint. Owing to symmetry, only one-quarter of the mirror model is used to carry out the FEA analyses. Because temperature distributions for schemes *B*, *C* and *D* are similar except that the value and location of the maximum temperature are slightly different, Fig. 4 shows temperature distributions only for schemes *A* and *D*.

When the length of the contact area is larger than that of the footprint, the maximum temperature is located at the centre of the footprint on a full mirror model, as shown in Fig. 4(*a*). If the length of the contact area is smaller than that of the footprint for schemes *B*, *C*

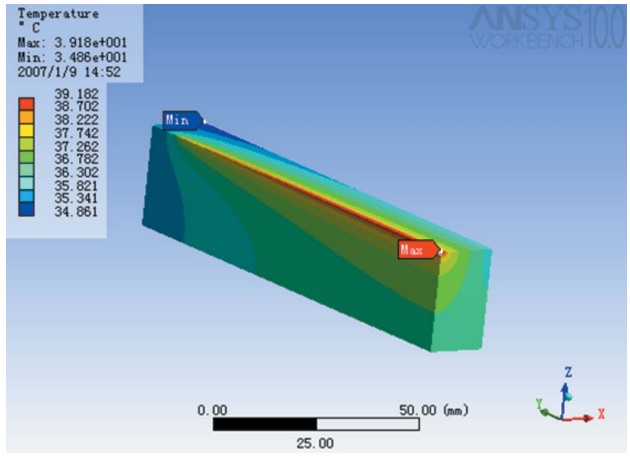

(*a*)

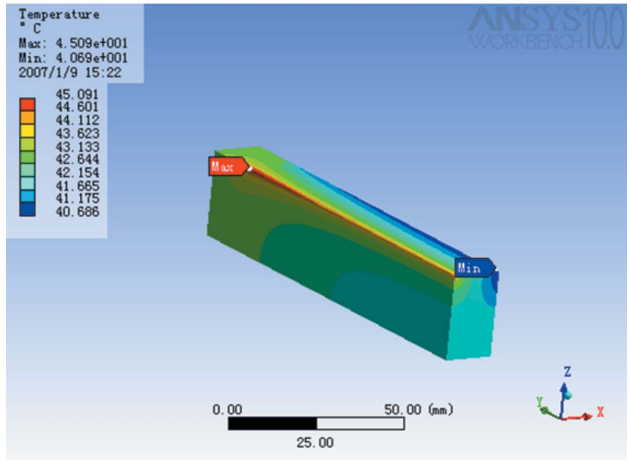

(*b*)

Figure 4
Three-dimensional temperature distributions for the one-quarter mirror model for schemes *A* (*a*) and *D* (*b*).

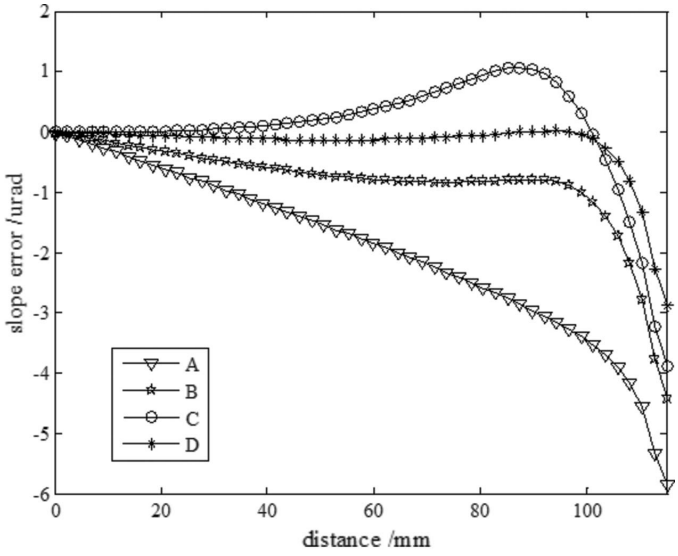

Figure 5
Slope error curve for the four schemes.

and *D*, the maximum temperature position moves away from the centre of the footprint along the *Y* direction, as shown in Fig. 4(*b*).

Four slope error curves are plotted in Fig. 5. Among the above four schemes, scheme *D* is the best one at present. Moreover, the slope error value in 90% of the footprint is smaller than 0.3 µrad and the RMS value for the whole footprint is only 0.569 µrad. It is clearly seen that the slope error is more uniform in scheme *D*, which is advantageous for the collimation mirror.

5. Structure of mechanical clamps

As mentioned above, the height of the contact area is very small (only 6 mm), so the structure of the cooling blocks, as shown in Fig. 6, is atypical. The cooling blocks are made of OFHC copper with a water-cooling channel. A 100 µm-thick indium foil between the upper part of the cooling block and the mirror is used for thermal contact. In Fig. 6 the small grid patterns indicate where 5 mm-thick Teflon is used for insulation, and are screwed together with a stainless steel frame.

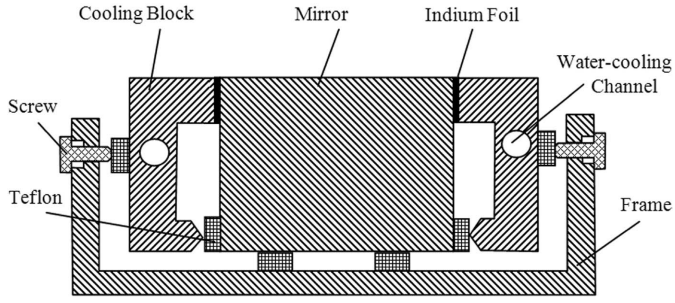

Figure 6
Cross-sectional view of a contact-cooled mirror.

6. Conclusion

A side-cooling method and optimization are described. This method has been used for a first-optical-element collimation mirror on the STXM beamline at the Shanghai Synchrotron Radiation Facility (SSRF). The thermal and structural performances of the optimized mirror are in agreement with design requirements. The mirror has been in operation since April 2009 and shows excellent performance.

We would like to express our appreciation to all the STXM beamline technicians for their help and support. This work has been supported by the National Natural Science Foundation of China under contract No.11175243.

References

ANSYS Inc. (2005). *ANSYS Workbench Documentation.* Release 10.0. ANSYS Inc., Canonsburg, PA, USA.
Artemev, A., Artemiev, N., Busetto, E., Hrdý, J., Mrazek, D., Plešek, I. & Savoia, A. (2001). *Nucl. Instrum. Methods Phys. Res. A*, **467–468**, 380–383.
Jaski, Y. R., Meron, M. & Viccaro, P. J. (1998). *Proc. SPIE*, **3447**, 62–71.
Khounsary, A., Yun, W., McNulty, I., Cai, Z. & Lai, B. (1998). *Proc. SPIE*, **3447**, 81–91.
Lee, W.-K., Fernandez, P. & Mills, D. M. (2000). *J. Synchrotron Rad.* **7**, 12–17.
Li, Y., Khounsary, A., Maser, J. & Nair, S. (2004). *Proc. SPIE*, **5193**, 204–210.
Zhang, L., Lee, W.-K., Wulff, M. & Eybert, L. (2003). *J. Synchrotron Rad.* **10**, 313–319.